MICHIGAN STATE UNIVERSITY

CYCLOTRON LABORATORY

ROTATIONAL BAND STRUCTURE IN N=105 AND 107 ISOTONES:

I. EVIDENCE FOR THE TRANSITION TO $|IRJ\rangle$ COUPLING AT HIGH SPINS IN ^{179}W.*

F. M. BERNTHAL AND R. A. WARNER

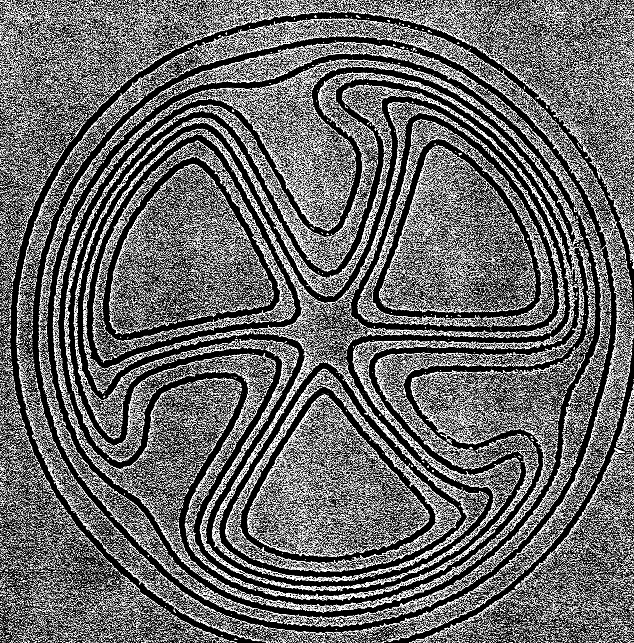

MAY 1974

MSUCL-114
COO-1779-142

COO-1779-142
MSUCL-114

Rotational Band Structure in N=105 and 107 Isotones:

I. Evidence for the Transition to $|IRJ\rangle$ Coupling at High Spins in ^{179}W

F. M. Bernthal and R. A. Warner

Departments of Chemistry and Physics and Cyclotron Laboratory,

Michigan State University, East Lansing, Michigan 48824

Keyword Abstract:

NUCLEAR REACTIONS: $^{177}Hf(\alpha,2n\gamma)$, E_α = 26 MeV, $^{181}Ta(p,3n\gamma)$, E_p = 26 MeV; Measured E_γ, I_γ, γ-γ coin. Enriched ^{177}Hf target. Deduced ^{179}W levels, I, π, K. Coriolis calculations, implied nuclear deformation, relevance to "backbending".

COO-1779-142
MSUCL-114

Rotational Band Structure in N=105 and 107 Isotones: I. Evidence for the Transition to |IRj> Coupling at High Spins in ^{179}W.*

F. M. Bernthal and R. A. Warner

Departments of Chemistry and Physics and Cyclotron Laboratory,

Michigan State University, East Lansing, Michigan 48824

ABSTRACT

The $^{177}Hf(\alpha,2n\gamma)$ and $^{181}Ta(p,3n\gamma)$ reactions have been employed in a study of the ^{179}W rotational band structure. Attention is focused on the unique-parity $9/2^+$[624] band and its highly-perturbed rotational structure. The higher spin members of the even-parity band in ^{179}W are not well-characterized by a single K quantum-number and are better represented in the |IRj> coupling scheme. Limits are placed on the hexadecapole deformation consistent with the rotational band structure in ^{179}W. The relevance of the even-parity band structure in ^{179}W to back-bending in neighboring even-A nuclei is discussed.

A. INTRODUCTION

Recent studies of rotational band structure in odd-A deformed rare-earth nuclei have contributed a wealth of new information on the so-called "parity-unique" Nilsson orbitals arising from the $h_{11/2}$ and $i_{13/2}$ shell-model states. The band structures of the respective odd-proton and odd-neutron orbitals associated with these states have typically been highly perturbed as a consequence of the large Coriolis matrix elements connecting the Nilsson orbitals of $\Omega' = \Omega \pm 1$.

It is of great interest to develop further the experimental systematics of the unique parity rotational bands for several reasons: (1) the single-particle structure associated with the transition from well-deformed to spherical nuclei has been poorly understood and indeed little investigated until most recently. Systematic studies of unique-parity band structures, with their known tendency toward decoupling of the odd particle from the rotation of the nuclear core at relatively modest rotational frequencies, offer an opportunity to study in the same nucleus band structure that is at once characteristic of well-deformed and of "transitional" nuclei. (2) Data on the marked increase in the yrast-band moment of inertia in even-even deformed nuclei at high rotational frequencies[1] have given rise to numerous attempts to explain the phenomenon. At least one of the explanations, that proposed by Stephens and Simon,[2] has features that depend on a correct understanding of the behaviour of the $i_{13/2}$ neutron orbitals in the presence of a rotating, deformed core. In particular, the frequently reported but still apparently unexplained attenuation of Coriolis matrix elements near the Fermi surface, required to reproduce in odd-mass nuclei the experimental energy spacing in rotational bands based on high-j Nilsson orbitals, is apparently essential to the understanding of the yrast states in even-even nuclei within the model of Ref. 2. Finally, (3) further data on isotopic and isotonic odd-A deformed nuclei may clarify the systematic changes in the ordering of the Nilsson single particle states as a function of quadrupole and hexadecapole deformation. It is to be hoped that rotational band structure and the rapidly-accumulating transfer-reaction data will provide a consistent picture of these deformation parameters and the strength of the Coriolis interaction.

The systematics of rotational band structure for the lower-Ω $i_{13/2}$ neutron orbitals are now relatively well-documented for the odd-A erbium and hafnium isotopes at least.[3,4] The general trend of the $5/2^+[642]$ and $7/2^+[633]$ bands in these isotopic series is toward increasing perturbation (and stronger Ω-mixture) as one moves toward the more neutron-deficient, less deformed species. Similar data for the higher-Ω $i_{13/2}$ orbitals in the $N \geq 105$ isotones are still relatively incomplete, however, and in view of the special importance of such data for the understanding of both odd-A and, it now appears, even-even species, it seems worthwhile to carry out a systematic study of the even-parity band structure in this region.

The $9/2^+[624]$ Nilsson state lies very near the ground state in the N=105 isotones ^{175}Yb, ^{177}Hf, ^{179}W, and presumably ^{181}Os, and is the ground state orbital of the N=107 isotones ^{177}Yb, ^{179}Hf, ^{181}W, and ^{183}Os. Extensive information on nuclear structure has already been deduced from a careful analysis of rotational band structure in ^{177}Hf populated by β-decay of the well-known 161-day isomer ^{177m}Lu.[4] Further useful information has been obtained on the $9/2^+[624]$ (ground) band in ^{179}Hf from decay of the 29-day isomer observed in that nucleus.[6] We have extended these data to the isotopes ^{179}W, ^{181}W, and ^{183}Os by in-beam γ-ray spectroscopy of the ^{177}Hf$(\alpha,2n\gamma)$, ^{180}Hf$(\alpha,3n\gamma)$, and ^{182}W$(\alpha,3n\gamma)$ reactions. The salient feature of these nuclei, i.e. the $9/2^+[624]$ band structure, has already been discussed in a preliminary way.[7] The general conclusion to be drawn from the data is that a relatively distinct $\Omega = 9/2$ structure in ^{177,179}Hf and ^{181}W gives way rather suddenly to a sharply perturbed structure in ^{179}W and ^{183}Os.

In this paper we report our results for the ^{179}W case and detail the results of Coriolis band-mixing calculations carried out on the $9/2^+[624]$ band structure in that nucleus. The data for this band in ^{179}W are, it seems, representative of the perturbations in the similar band structure in ^{183}Os in the same way that the ^{177}Hf data parallel the ^{181}W data (Fig. 1). The details of our ^{181}W and ^{183}Os experiments will be reported separately.

B. EXPERIMENTAL

A thick chip of separated isotope ^{177}Hf metal (92% enriched) was suspended on a 1/4-mil Ta wire and bombarded with 26-MeV α-particles from the Michigan State University Sector-focused Cyclotron to obtain the $(\alpha,2n)$ reaction product ^{179}W. The γ-ray spectra were obtained with a 2.5%-efficient Ge(Li) detector with 2.3 keV (FWHM) resolution at 1333 keV. The spectrum of prompt γ-rays seen in the ^{177}Hf$(\alpha,2n\gamma)^{179}$W reaction is shown in Fig. 2. Because the target used in this experiment was thick, the

$(\alpha, n\gamma)^{180}W$ lines also appear prominently in the spectrum. In addition to the singles data, in-beam γ-γ coincidence data were gathered in an experimental configuration that included a 6.5% Ge(Li) detector as well as the smaller 2.5% device. Resolving time of the coincidence system was about 15 nsec (FWHM), though the effective resolving time was limited by the cyclotron duty cycle to ∿60 nsec. As the thick ^{177}Hf target used in this experiment complicated the acquisition of meaningful γ-ray anisotropy data, a $^{181}Ta(p,3n\gamma)$ cross-bombardment was carried out to provide an additional check on the γ-rays assigned to ^{179}W in the $(\alpha, 2n)$ experiment. Singles and coincidence data were also gathered in the $^{181}Ta(p,3n\gamma)$ experiment. The results correlated well in all respects with the conclusions of the $(\alpha, 2n)$ work.

C. RESULTS

Fig. 3 shows the level structure of ^{179}W deduced from the γ-ray singles data of Fig. 2, and from the γ-γ coincidence data. The level scheme is consistent with the earlier $^{179}Re \rightarrow {}^{179}W$ decay data of Arlt, *et al.*[8] and with the (d,p) and (d,t) reaction data of Casten, *et al.*[9] The most noteworthy feature of the level scheme is the large perturbation associated with the even-parity band. The presence of the $7/2^+[633]$ state at 477.4 keV, only 168 keV from the $9/2^+[624]$ band head, makes the assignment of a K-quantum number to the even-parity band moot. The strong perturbation of the even-parity band and the consequent difficulty in ordering the lower-lying members of that band is undoubtedly responsible for the discrepancy which exists between our data and the preliminary $^{181}Ta(p,3n\gamma)$

data of Konijn, *et al.*[10] The $(p,3n\gamma)$ work has recently been repeated by Birattari, *et al.*,[11] but this group only reported their assignments to the $7/2^-[514]$ (ground) and $1/2^-[521]$ (221.9-keV) bands. The recent results from the $^{178}Hf(\alpha,3n\gamma)$ and $^{181}Ta(p,3n\gamma)$ experiments reported by the Stockholm group[12] corroborate our level scheme in every respect.

The key to the correct ordering of the even-parity band members is to be found in the 253.0-keV coincidence data of Fig. 4. These data are to be compared with the 189.1-keV $9/2^+ \rightarrow 9/2^-$ coincidence data. The 253-keV line is clearly in coincidence with the even-parity band members. The 63.9-keV energy difference correlates well with the 63.88-keV transition reported by Konijn, *et al.* on the basis of their bent crystal γ-ray data.[13] In addition, the anisotropy of the 253-keV line is found in our $(p,3n\gamma)$ data to be consistent with a dipole assignment for this γ-ray.

Also shown in Fig. 4 are sample coincidence data for crossover stretched quadrupole transitions in the $7/2^-[514]$ and $9/2^+[624]$ bands.

In the $^{181}Ta(p,3n\gamma)$ experiment, no new information on the ^{179}W level structure was obtained, but data were taken with a small Ge(Li) diode (16 mm dia.×5 mm. deep) having resolution ∿600 eV FWHM at 122 keV. These data permitted us to resolve the 96-keV doublet as shown in Fig. 5. The lower-energy component (95.89 keV) is placed by energy difference as the $13/2^+ \rightarrow 11/2^+$ cascade transition in the even-parity band, while the high-energy component (96.58 keV) is the $5/2^- \rightarrow 1/2^-$ transition in the $1/2^-$ [521] band.

Table I summarizes the γ-ray data obtained in the $^{177}Hf(\alpha,2n\gamma)$ experiment.

D. DISCUSSION

1. Limits to Deformation for ^{179}W

It is the primary intent of this note to deal further with the perturbed even-parity band structure in ^{179}W. We need not detail the band-fitting results also reported by the Stockholm group. With the higher angular momentum available in the $^{179}Hf(\alpha,3n\gamma)$ reaction, Lindblad *et al.*[12] are able to identify states to spin 29/2 in the even parity band of ^{179}W. By a reasonable choice of deformation parameters and rotational constants, and with a suitable *ad hoc* attenuation of Coriolis matrix elements near the Fermi surface, they are able to fit the rotational band within ±1.0 keV of experiment for all known even-parity states in ^{179}W. In our calculations, we employ a similar diagonalization of the Coriolis interaction matrix. The diagonal and off-diagonal elements are

$$(1) \qquad E^{diag}_{Rot} = \left\{\frac{\hbar^2}{2J} + B[I(I+1)-K^2]\right\} \left[I(I+1)-K^2 + (-1)^{I+\frac{1}{2}} a(I+\tfrac{1}{2})\delta_{K,\frac{1}{2}}\right]$$

and

$$(2) \qquad E_{RPC} = -\left[\frac{\hbar^2}{2J} + B\ I(I+1)\right] \sqrt{I(I+1)-K_>K_<}\ \langle j\Omega|j_{\mp}|j,\Omega\pm1\rangle \times N_{\Omega,\Omega+1} \times R(U,V)$$

Where $N_{\Omega,\Omega+1}$ is an *ad hoc* factor, and R(U,V) is the usual pairing reduction factor, $(U_\Omega U_{\Omega+1} + V_\Omega V_{\Omega+1})$. The diagonalization is carried out with use of a minimization routine which allows one to vary simultaneously and independently any of the off-diagonal or diagonal matrix elements. It is reassuring to note that, when we allow all Coriolis matrix elements, the $9/2^+[624]$ quasiparticle energy, and the parameters $\hbar^2/2J$ and B to vary simultaneously, we arrive at a parameter set that differs insignificantly from the more constrained set of Ref.[12]

While this agreement may instill some degree of confidence in the band-fitting procedure, it seemed worthwhile to experiment with the input spectrum of quasiparticle energies in an attempt to determine just how sensitive the results are to the assumed deformation. This exercise is expecially desirable in view of recent reports[14,15] that suggest hexadecapole deformations in the Hf and W isotopes considerably larger than those indicated by the calculations of Nilsson, *et al.*[16]

Consequently, we have tried to determine the limits of deformation, and the associated quasiparticle input energies for which one is able still to obtain physically reasonable fits to the experimentally observed even-parity states in ^{179}W. In this procedure, we have calculated the average field single particle energies with use of the code of Nilsson *et al.*[16] and the pairing reduction factors R(U,V) in equation 2, though usually not significantly smaller than unity, have been estimated with use of the expression.

$$V_\Omega^2 = 1/2 \left[1 - \frac{\varepsilon_\Omega - \lambda}{E_\Omega} \right]$$

The chemical potential, λ, is chosen on the basis of the best empirical evidence (cf. Ref. 17), and the gap parameter Δ is taken from Ref. 16. The diagonal quasiparticle energies are thus

$$E_{\nu}^{\Omega} = \sqrt{(\varepsilon_{\Omega}-\lambda)^2 + \Delta_{\nu}^2}$$

where E_{Ω} is the Nilsson single particle energy for a given Ω-state.

The results of this investigation are shown in Table II. The criterion used for goodness of fit, $\Sigma(\Delta E)^2$, is extremely sensitive, so that in view of the uncertainty in the energy of the second $13/2^+$ state and of the highest spin states, the precision of the various fits is relatively similar. The fit shown in each case represents the optimum that could be achieved after repeated attempts with various constraints on the minimization routine. The qualitative information conveyed by each fit is not significantly changed by any amount of realistic parameter juggling. Many of the variations between the different parameter sets are in fact quite transparent; the tendency of the minimization routine to try to compensate for too small a value of ε_4 is evident, for example, in the increased size of the off-diagonal matrix elements for small values of Ω. While the details of each fit may be debatable (for example, one may prefer to use a smooth attenuation function[2,12] for the Coriolis matrix elements), the fitting parameters generally do not strain credibility until ε_4 is allowed to reach or exceed 0.08.

It seems clear then, *for a sufficient number of experimental data points*, it is possible to differentiate between deformation parameters on the basis of rotational band structure. The emphasis above is important, as shown in the case of the calculations for $\varepsilon_4 = 0.08$. The location of the second $13/2^+$ state from transfer reaction data (unfortunately, the energy is known only to ±6 keV) provides a critical constraint on the allowable input quasiparticle spectrum. If one does not require the second $13/2^+$ state to be fit, relatively good fits to the remaining experimental data can be obtained, though the off-diagonal elements are evidently difficult to understand even if that requirement is removed. This fact points again to the great desirability of obtaining further experimental data on the quasiparticle spectrum of such nuclei. While transfer reaction data have provided much useful information in this regard, it is also true that in many cases detailed decay studies provide means of identifying the various Nilsson states. Though the decay of ^{179}Re (20 min.) has been studied by several investigators,[18,19] further decay work on this and other odd-N nuclei in this region should yield important new data.

From the limited available data, however, we can draw some general conclusions about the band-fitting procedure in ^{179}W:

(a) Generally speaking, one can select a set of physically realistic moment of inertia and Coriolis matrix element parameters to fit the even-parity states of ^{179}W reasonably well for nearly any deformation from $\varepsilon_2 = 0.20-0.26$ and $\varepsilon_4 = 0.00-0.06$.

(b) For *any* set of input quasiparticle energies included in our calculations, the phenomenon of large attenuation of the off-diagonal matrix elements near the Fermi surface continues to be evident. This effect has been profusely noted,[5,12,21,22] but to date has not been satisfactorily explained.

(c) It is significant that it seems *not* to be possible to fit the experimental data if one assumes an input quasiparticle spectrum that would correspond to $\varepsilon_4 \geq 0.08$. One might hope, therefore, to be able to make some distinction between the systematically larger values for hexadecapole deformation that seem to arise from Coulomb excitation measurements as compared to the values implied by inelastic scattering from the nuclear potential.[14]

The problem of hexadecapole deformation measurements has been discussed in some detail by Hendrie,[14] and for the region around A = 180 it has become strikingly apparent with the recent results of Bemis *et al.*[15] The Oak Ridge group finds $\beta_4 = -0.18 \pm 0.06$ for ^{182}W, a measurement obtained by Coulomb excitation with alpha particles. While the sensitivity of their β_4 result to incident α-particle energy may account for a major portion of the large discrepancy,[15] the possibility that the proton and neutron distributions at the nuclear surface are different cannot be ruled out.

In marked contrast to the Oak Ridge result are the recent data of Davidson *et al.*[20] Their analysis of muonic x-ray energies for a number of deformed rare-earth and actinide nuclides shows relatively good agreement with the values of β_4 determined from α-scattering and Coulomb excitation, except for the ^{182}W case, where the muonic x-ray results indicate $\beta_4 \cong 0$.

Further experimental work on the deformation systematics in the A = 180 region is certainly needed; for the moment however, it is difficult to see how the data on rotational structure based on the even-parity $i_{13/2}$ neutron orbitals in this region can be reconciled with hexadecapole deformations much in excess of $\varepsilon_4 = 0.06$ (i.e. $\beta_4 = -0.05$ for $\varepsilon_2 \cong 0.25$). One might also note that the $i_{13/2}$ neutrons should if anything contribute *more* to the second-order fluctuations in the shape of the nuclear surface than should the lower-N orbitals, and therefore should be good indicators of the hexadecapole deformation to be expected in this region.

2. Implications of Even-parity Band Structure for "Backbending"

The relevance of rotational band structure in odd-A nuclei to the phenomenon of "backbending" observed in numerous even-even nuclei has been noted. Stephens has proposed that the tendency of the $i_{13/2}$ neutrons to decouple from the nuclear core rotation may be indicated for even-even nuclei by the similarity of the ground-band 0^+-2^+ energy spacing in those nuclei to the $13/2^+$ - $17/2^+$ spacing in neighboring odd-A species.[23,24] In their most recent manuscript, Stephens *et al.*[24] show that the tendency toward backbending near the "rare earth" deformed region can by the above procedure be predicted in a general way, although the results for the W and Os region are less than conclusive.

A fundamental and quantitative measure of the approach toward particle-core decoupling can be easily obtained with use of the eigenvectors obtained from diagonalization of the complete Coriolis interaction matrix as carried out in this study. The expansion coefficients in Ω for each spin state can then be used to determine the expectation value for R, the nuclear core rotation, in the $|IRj\rangle$ coupling scheme of Vogel:[25]

$$(3) \quad |IRj\rangle = \sqrt{\frac{2I+1}{8\pi^2}} \sum_{\Omega=-j}^{+j} (-1)^{j-\Omega}(Ij\Omega{-}\Omega|R0) \times \mathcal{D}^{I}_{M\Omega} \, |j\Omega\rangle$$

The expansion coefficients for a state of spin I in the $|IRj\rangle$ representation are then easily found from the overlap of the expression (3) with the conventional wave function for an axially symmetric nuclear rotation superimposed on an intrinsic state with projection Ω:

$$(4) \quad |I\Omega\rangle = \sqrt{\frac{2I+1}{16\pi^2}} \sum_{\Omega>0} f^{I}_{\Omega} \left[\mathcal{D}^{I}_{M\Omega}\chi_{\Omega} + (-1)^{I-\Omega}\mathcal{D}^{I}_{M-\Omega}\chi_{-\Omega}\right]$$

where the f^{I}_{Ω} are the expansion coefficients in Ω obtained from solution of the Coriolis secular determinant. The overlap of (3) and (4) then yields[25]

$$(5) \quad \langle IRj|I\Omega\rangle = \sqrt{2} \sum_{\Omega=\frac{1}{2}}^{j} (Ij\Omega{-}\Omega|R0) f^{I}_{\Omega} C^{\Omega}_{j\ell}$$

where the $C^{\Omega}_{j\ell}$ are the usual coefficients defining the eigenfunction for solution of the Nilsson single particle Hamiltonian in the spherical harmonic oscillator basis. For a given spin, the expectation value $\langle R\rangle$ may be conveniently calculated as

$$(6) \qquad \langle R \rangle = \sum_R \left[\langle IRj | I\Omega \rangle \right]^2 R$$

where R is restricted to even integral values.

By calculating $\langle R \rangle$ for various odd-A nuclei in the "rare-earth" region, we have been able to demonstrate the expected high correlation between tendency of the $i_{13/2}$ particle to decouple from the core rotation and the appearance of "backbending" phenomena in neighboring even-even nuclei.[26] The results of this study are in qualitative agreement with the concurrent study of Stephens *et al.*[24] though some differences are apparent for the W-Os region.

For the ^{179}W case of interest here, it is useful to compare the degree of decoupling with that in other odd-N species. In Fig. 6, the quantity $[\langle R \rangle - R_{min}]$ is plotted as a function of spin for several deformed nuclei. The value R_{min} represents the minimum (decoupled) value for the nuclear core rotation, so that in the limit of complete decoupling, the quantity plotted should approach zero, if one assumes a pure $i_{13/2}$ wave-function for the Nilsson state. (It does not in Fig. 6 because the $g_{9/2}$ component in some cases approaches 10% of the wave-function.)

In ^{179}W, even at spin 13/2, the "$\Omega = 9/2$" band is found to be about 50% $|IRj\rangle = |13/2\ 0\ 13/2\rangle$ character, and the expectation value for R is quite low, 1.95ħ. The significance of this number can be seen by comparing it with the Er and Hf cases included in Fig. 6. In a well-known backbending region, the even-parity $i_{13/2}$ band in ^{163}Er is found to have $\langle R \rangle = 1.74\hbar$. In contrast, for ^{177}Hf $\langle R \rangle = 3.14\hbar$ for spin 13/2. The neighboring even-

even species ^{176}Hf shows little evidence for backbending[28] up to spin 18 and, though less meaningful, the same can be said for ^{178}Hf to spin 12.

Thus, surprisingly enough, the possible role of $i_{13/2}$ neutrons in the backbending phenomenon in even-even W and Os isotopes[29] cannot be dismissed out of hand. The increasingly large rotational constant $\hbar^2/2J$, and the large hexadecapole moments in this region work to destroy the higher degree of adiabaticity otherwise expected for the high-Ω $i_{13/2}$ particles. It appears from the calculations summarized in Fig. 6 that if the Stephens-Simon picture is valid for explaining the backbending effect in ^{162}Er and ^{164}Er, then it should also apply to the W - Os region. Further work on the yrast structure in this region is in progress in our laboratory.

While it may be attractive to hope that all backbending in the rare-earth region can be blamed on the intrusion of decoupled $i_{13/2}$ neutron two-quasiparticle band structures into the yrast sequence, it also seems clear that the more general phenomena observed in the near-deformed regions will require substantially more data and perhaps a variety of theoretical approaches before one can advance a comprehensive explanation of high-spin phenomena in "deformed" and "shell-model" nuclei.

E. ACKNOWLEDGEMENTS

We wish to thank Professors Wm. C. McHarris and W. H. Kelly for their support and interest in initiating this work. We also thank Dr. R. R. Todd, Dr. L. F. Samuelson, and Ms. C. L. Dors for their assistance. The comments and suggestions of Drs. T. L. Khoo and P. Vogel have been most helpful.

APPENDIX

Considerable confusion exists in transforming nuclear deformations expressed in terms of β_2, β_4 ... to deformations expressed as ε_2, ε_4 ... . The former representation specifies the coordinates of the nuclear radius defined by the expansion in spherical harmonics

$$R = R_0(1 + \beta_2 Y_{20} + \beta_4 Y_{40} + \beta_6 Y_{60} + \ldots)$$

while the latter is used to characterize the deformed oscillator potential.[16] Because of the unusually large hexadecapole moments that have recently been associated with W and Os nuclei, it seems appropriate to provide a short table relating the two deformation parameters. Dr. C. F. Tsang has kindly provided us with a code which transforms deformations in the ε representation to the β coordinate system. More extensive tables and graphs will be published elsewhere by Tsang, Nilsson and Möller.[30]

REFERENCES

* Work supported by the U.S. Atomic Energy Commission and by the National Science Foundation.

1. A summary of experimental data is given by R. A. Sorensen, Rev. Mod. Phys. 45, 353 (1973).

2. F. S. Stephens and R. S. Simon, Nucl. Phys. A138, 257 (1972).

3. S. A. Hjorth, H. Ryde, K. A. Hagemann, G. Lovhoiden, and J. C. Waddington, Nucl. Phys. A144, 513 (1970).

4. S. Hultberg, I. Rezanka, and H. Ryde, Nucl. Phys. A205, 321 (1973).

5. F. M. Bernthal and J. O. Rasmussen, Nucl. Phys. A101, 513 (1967).

6. H. Hubel, R. A. Naumann, M. L. Andersen, J. S. Larsen, O. B. Nielsen, and N. O. Roy Poulsen, Phys. Rev. C1, 1845 (1970).

7. F. M. Bernthal and R. A. Warner, Bull. Am. Phys. Soc. 16, 1146 (1971), F. M. Bernthal, R. A. Warner, and R. W. Goles, Bull. Am. Phys. Soc. 17, 584 (1972); F. M. Bernthal, R. A. Warner, and C. L. Dors, Bull. Am. Phys. Soc. 17, 900 (1972); J. S. Boyno, F. M. Bernthal, T. L. Khoo, and R. A. Warner, Bull. Am. Phys. Soc. 18, 1405 (1973). See also Michigan State University Cyclotron Laboratory Annual Report 1972-73.

8. R. Arlt, K. Ya Gromov, N. G. Zaitseva, Li Chun Khi, Z. Malek, G. Musiol, and H. Strusny, Isv. Akad, Nuak SSSR, Ser. Fix. 34, (1970) [transl.: Bull. Acad. Sci. USSR, Phys. Ser. 34, 619 (1970.]

9. R. F. Casten, P. Kleinheinz, P. J. Daly, and B. Elbek, Mat. Fys. Medd. Dan. Vid. Selsk. 38, No.13 (1972).

10. J. Konijn, B. Klank, J. H. Jett, and R. A. Ristenen, *Contributions to the International Conference on Properties of Nuclear States, Montreal, 1969*, p. 77.

11. C. Birattari, A. M. Grassi Strini, G. Lo Bionco, G. Strini, and G. Tagliaferri, *Contribution to the Conference on High Spin Nuclear States and Related Phenomena, Stockholm, 1972.*

12. Th. Lindblad, H. Ryde, and P. Kleinheinz, Nucl. Phys. A201, 369 (1973).

13. J. Konijn, B. Klank, J. H. Jett, and R. A. Ristenen, Bull. Am. Phys. Soc. 14, 509 (1969) and private communication.

14. D. L. Hendrie, Phys. Rev. Lett. 31, 478 (1973).

15. C. E. Bemis, P. H. Stelson, F. K. McGowan, W. T. Milner, J. L. C. Ford, Jr., R. L. Robinson, and W. Tuttle, Phys. Rev. C, 8, 1934 (1973).

16. S. G. Nilsson *et al.*, Nucl. Phys. A131, (1969).

17. W. Ogle, S. Wahlborn, R. Piepenbring, and S. Fredriksson, Rev. Mod. Phys. 43, 424 (1971).

18. R. Arlt, K. Ya. Gromov, N. G. Zaitseva, Li Chun Khi, Z. Malek, G. Musiol, and H. Strusny, Bull. Acad. Sci. USSR (Phys. Ser.) [trans.: 34, 619 (1970).]

19. B. Harmatz and T. H. Handley, Nucl. Phys. A121, 481 (1973).

20. J. P. Davidson, D. A. Close, and J. J. Malanify, Phys. Rev. Lett. 32, 337 (1974).

21. F. S. Stephens, M. D. Holtz, R. M. Diamond, and J. O. Newton, Nucl. Phys. A115, 129 (1968).

22. F. S. Stephens, University of California Report No. LBL-1251, (1972) unpublished.

23. F. S. Stephens, *Proceedings of the International Conference on Nuclear Physics*, Vol. 2 (ed. J. deBoer and H. J. Mang), North-Holland (1973) p. 368.

24. F. S. Stephens, P. Kleinheinz, R. K. Sheline, and R. S. Simon, Lawrence Berkeley Laboratory Report LBL-1911 (1973).

25. P. Vogel, Phys. Lett. 33B, 400 (1970).

26. F. M. Bernthal - to be published.

27. H. Hübel, R. A. Naumann, M. L. Andersen, J. S. Larsen, O. B. Nielsen, and N. O. Roy Poulson, Phys. Rev. C 1, 1845 (1970).

28. T. L. Khoo and F. M. Bernthal - to be published.

29. R. A. Warner, F. M. Bernthal, J. S. Boyno, T. L. Khoo, and G. Sletten, Phys. Rev. Lett. 31, 835 (1973).

30. C. F. Tsang, S. G. Nilsson, and P. Möller, Atomic and Nucl. Data - to be published.

Table I. Energies and Relative Intensities of γ-rays Assigned to ^{179}W from the $^{177}Hf(\alpha,2n\gamma)$ Reactions

E_{γ}(keV)[a]	I_{γ}[b]	Assignment: I_i^{π} → I_f^{π}	Assignment: Band Placement
82.94	4.6	$3/2^- \rightarrow 1/2^-$	$1/2^-$[521]
95.89	21 (95.89 + 96.58)	$13/2^+ \rightarrow 11/2^+$	$9/2^+$[624]
96.58		$5/2^- \rightarrow 1/2^-$	$1/2^-$[521]
108.43	5.7(6)	$11/2^+ \rightarrow 11/2^-$	$9/2^+$[624] → $7/2^-$[514]
119.96	≡100	$9/2^- \rightarrow 7/2^-$	$7/2^-$[514]
137.6[c]	24[c]	$15/2^+ \rightarrow 13/2^+$	$9/2^+$[624]
142.25	14	$17/2^+ \rightarrow 15/2^+$	$9/2^+$[624]
144.68	13	$11/2^- \rightarrow 9/2^-$	$7/2^-$[514]
159.94	7.4	$13/2^+ \rightarrow 9/2^+$	$9/2^+$[624]
162.5(2)	3.5	$21/2^+ \rightarrow 19/2^+$	$9/2^+$[624]
168.3[d]	8.2[d]	$7/2^+ \rightarrow 9/2^+$	$7/2^+$[633] → $9/2^+$[624]
		$13/2^- \rightarrow 11/2^-$	$7/2^-$[514]
189.1	126[d] (189.1 + 190.5)	$9/2^+ \rightarrow 9/2^-$	$9/2^+$[624] → $7/2^-$[514]
190.5(2)		$15/2^- \rightarrow 13/2^-$, $7/2^- \rightarrow 5/2^-$	$7/2^-$[514] and $1/2^-$[521]
204.20	22	$7/2^- \rightarrow 3/2$	$1/2^-$[521]
211.34(8)	2.5(3)	$17/2^- \rightarrow 15/2^-$	$1/2^-$[521]
212.79	7.0	$19/2^+ \rightarrow 17/2^+$	$9/2^+$[624]
214.91	25	$9/2^- \rightarrow 5/2^-$	$1/2^-$[521]
221.99	9.1	$1/2^- \rightarrow 7/2^-$	$1/2^-$[521] → $7/2^-$[514]
233.3(2)[e]	28(10)[f]	$15/2^+ \rightarrow 11/2^+$	$9/2^+$[624]
252.96	42	$11/2^+ \rightarrow 9/2^-$	$9/2^+$[624] → $7/2^-$[514]

Table I - continued

264.63	66	$11/2^- \to 7/2^-$	$7/2^-[514]$
279.73	31	$17/2^+ \to 13/2^+$	$9/2^+[624]$
309.03	85	$9/2^+ \to 7/2^-$	$9/2^+[624] \to 7/2^-[514]$
312.77	45	$13/2^- \to 9/2^-$	$7/2^-[514]$
314.66	9.8	$11/2^- \to 7/2^-$	$1/2^-[521]$
323.79	22	$13/2^- \to 9/2^-$	$1/2^-[521]$
354.95	21	$19/2^+ \to 15/2^+$	$9/2^+[624]$
358.51	36	$15/2^- \to 11/2^-$	$7/2^-[514]$
375.10	16	$21/2^+ \to 17/2^+$	$9/2^+[624]$
401.6[d]	30	$17/2^- \to 15/2^-$ $15/2^- \to 11/2$	$7/2^-[514]$ $1/2^-[521]$
415.78	15	$17/2^- \to 13/2$	$1/2^-[521]$
430.2[g]	22	$5/2^- \to 7/2^-$?	$5/2^-[512] \to 7/2^-[514]$?
441.64	16	$19/2^- \to 15/2^-$	$7/2^-[514]$
459.9	3.8	$25/2^+ \to 21/2^+$	$9/2^+[624]$
464.4	9.1	$23/2^+ \to 19/2^+$	$9/2^+[624]$
477.4	17	$21/2^- \to 17/2^-$	$7/2^-[514]$
478.7	8.4	$19/2^- \to 15/2^-$	$1/2^-[521]$
482.5	4.9	$21/2^- \to 17/2^-$	$1/2^-[521]$
511.8(7)[h]	(8)	$23/2^- \to 19/2^-$	$7/2^-[514]$
541.6	3	$25/2^- \to 21/2^-$	$7/2^-[514]$

Footnotes to Table 1.

[a] Unless otherwise indicated (parentheses), energy errors may be taken as ±0.10 keV where two decimal digits are given, and ± 0.2 keV where only one decimal digit is given.

[b] Except as otherwise noted, relative intensity errors are ±8%.

[c] Doublet includes ^{177}Hf Coulomb excitation line at 137.0 keV.

[d] Unresolved doublet. Relative intensity is the sum of the line intensities.

[e] Energy taken from (*p*,3*n*γ) data.

[f] Relative intensity estimated from coincidence data. Line obscured by ^{180}W $4^+ \to 2^+$ g.r.b. transition.

[g] Line apparently belongs to ^{179}W, and possibly is associated with the $5/2^-$[512] state at 430 keV identified by Casten *et al.*[9] However, we are unable to confirm this assignment from coincidence data that should be associated with the $5/2^-$[512] band.

[h] Energy and relative intensity from coincidence data (see Fig. 4).

Table II. Results of Energy Fits to Even-Parity States in ^{179}W from Diagonalization of Coriolis Interaction Matrix

ε_2	ε_4	$\Sigma(\Delta E)^2$ (keV^2)[a]	$\hbar^2/2J$ (keV)	B (eV)	Attenuation Factors[b] 1/2×3/2	3/2×5/2	5/2×7/2	7/2×9/2	9/2×11/2	$[E_{9/2^+} - E_{7/2^+}]$[c] (keV)
0.20	0.	0.13	18.0	-9.3	1.08	0.98	0.91	0.67	0.70	165
0.22	0.	0.05	18.7	-10.	1.19	1.03	1.01	0.64	0.75	182
0.22	0.04	0.17	17.5	-8.9	1.01	0.91	0.91	0.61	0.59	155
0.22	0.08	18.[d]	17.5	-12.	0.79	0.22	1.13	0.39	1.05	305
0.24	0.00	0.01	19.4	-11.	1.30	1.06	1.10	0.60	0.76	192
0.24	0.04	0.26	17.6	-9.2	0.98	0.93	0.91	0.59	0.73	155
0.24	0.08	6.6[d]	17.4	-11.	0.87	0.34	1.14	0.34	1.06	302
0.26	0.00	30.	19.0	-6.9	1.39	1.16	1.09	0.62	0.77	180
0.26	0.04	0.06	18.1	-10.	1.12	0.95	1.02	0.56	0.62	175
0.26	0.08	3.0[d]	17.5	-10.	0.97	0.48	1.18	0.33	1.04	398

[a] Sum of the squares of differences between experimental and fitted energies for all even-parity states shown in Fig. 3, and for $27/2^+$ and $29/2^+$ data from Ref. 12 (1987.7 and 2121.0 keV), and second $13/2^+$ state at 914 ± 6 keV (Ref. 9).

[b] Attenuation factors $N_{\Omega,\Omega+1}$ for off-diagonal matrix elements required to achieve indicated fit to experimental data. The relatively insensitive 11/2 × 13/2 matrix element was kept constant at the unattenuated value.

[c] The $9/2^+$[624] quasiparticle energy is allowed to vary relative to the other $i_{13/2}$ Nilsson orbitals. While these variations are relatively small with respect to the precision that one has a right to expect from the Nilsson model after correction for pairing, they do allow a more satisfactory fit to the experimental data. The remaining quasi-

particle energies are those obtained from the program of Nilsson *et al.*,[15] assuming $\lambda = [\varepsilon_{7/2^-[514]} + 150$ keV) and $\Delta = 900$ keV.

[d] Unable to fit second $13/2^+$ state ($\simeq$914 keV). If that constraint is applied $\Sigma(\Delta E)^2 \cong 10^4$.

Table III. Table for Transforming Deformation Parameters from ε_2, ε_4 to β_2, β_4, β_6 Representation

ε_2	ε_4	β_2	β_4	β_6	ε_2	ε_4	β_2	β_4	β_6
0.16	0.00	0.17	0.011	0.00	0.22	0.00	0.24	0.021	0.00
	0.04	0.17	-0.037	-0.01		0.04	0.24	-0.028	-0.01
	0.08	0.18	-0.085	-0.01		0.08	0.25	-0.076	-0.02
	0.12	0.18	-0.13	-0.02		0.12	0.25	-0.12	-0.03
	0.16	0.19	-0.18	-0.02		0.16	0.25	-0.17	-0.04
	0.20	0.20	-0.22	-0.03		0.20	0.26	-0.21	-0.04
0.18	0.00	0.19	0.014	0.00	0.24	0.00	0.26	0.025	0.00
	0.04	0.20	-0.035	-0.01		0.04	0.26	-0.024	-0.01
	0.08	0.20	-0.082	-0.02		0.08	0.27	-0.071	-0.02
	0.12	0.20	-0.13	-0.02		0.12	0.27	-0.12	-0.03
	0.16	0.21	-0.18	-0.03		0.16	0.28	-0.16	-0.04
	0.20	0.22	-0.22	-0.03		0.20	0.29	-0.21	-0.05
0.20	0.00	0.22	0.017	0.00	0.26	0.00	0.28	0.017	0.00
	0.04	0.22	-0.031	-0.01		0.04	0.29	-0.019	-0.01
	0.08	0.22	-0.079	-0.02		0.08	0.29	-0.067	-0.02
	0.12	0.23	-0.13	-0.03		0.12	0.30	-0.11	-0.03
	0.16	0.23	-0.17	-0.03		0.16	0.30	-0.16	-0.04
	0.20	0.24	-0.22	-0.04		0.20	0.31	-0.21	-0.05

FIGURE CAPTIONS

Fig. 1 Plot of [$E(I \rightarrow I-1)/2I$] vs. $2I$ for the $9/2^+[624]$ bands in N=105 and 107 isotones. In the normal rotational energy expansion $E = E_0 + \hbar^2/2\mathcal{J}[I(I+1)] + BI^2(I+1)^2$, such a plot has slope B and intercept $\hbar^2/2\mathcal{J}$. Data for ^{177}Hf are from Refs. 4 and 5 and the ^{183}Os data are from our laboratory.[7]

Fig. 2 Singles prompt γ-ray spectrum seen in the $^{177}Hf(\alpha,2n\gamma)^{179}W$ reaction at E_α = 26 MeV.

Fig. 3 The level scheme of ^{179}W deduced from $^{177}Hf(\alpha,2\ \gamma)^{179}W$ data. Transitions labeled with an asterisk are unresolved from other lines.

Fig. 4 The 189-, 253-, 280-, and 358-keV gated γ-γ coincidence spectra from $^{177}Hf(\alpha,2n\gamma)^{179}W$.

Fig. 5 Portion of the $^{181}Ta(p,3n\gamma)$ spectrum showing resolution of 96-keV doublet in ^{179}W.

Fig. 6 The value $[\langle R\rangle - R_{min}]$ (see text) for the nuclear core rotation as a function of spin for the even-parity band in ^{179}W. Shown for comparison are data for ^{161,163,165}Er (Ref. 3) and ^{177}Hf (Ref. 4) and ^{179}Hf (Ref. 27). Negative values occur at high spins because the single-particle wave-function is not pure $i_{13/2}$.

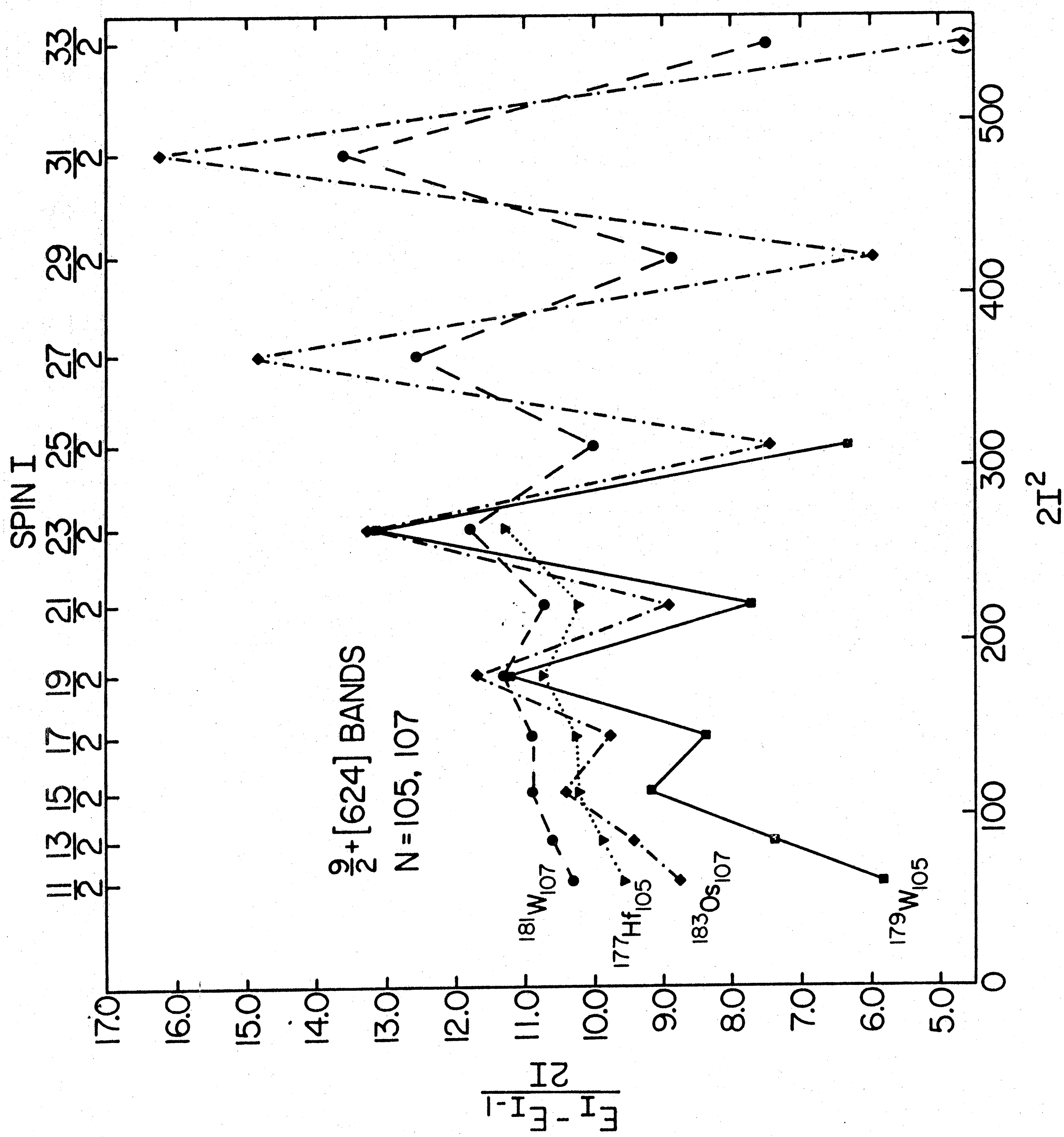
SPIN I
11/2
13/2
15/2
17/2
19/2
21/2
23/2
25/2
27/2
29/2
31/2
33/2
9/2+[624] BANDS
N=105, 107
181W107
177Hf105
183Os107
179W105
17.0
16.0
15.0
14.0
13.0
12.0
11.0
10.0
9.0
8.0
7.0
6.0
5.0
0
100
200
300
400
500
2I^2
(E_I - E_I-1)/2I

Fig. 1

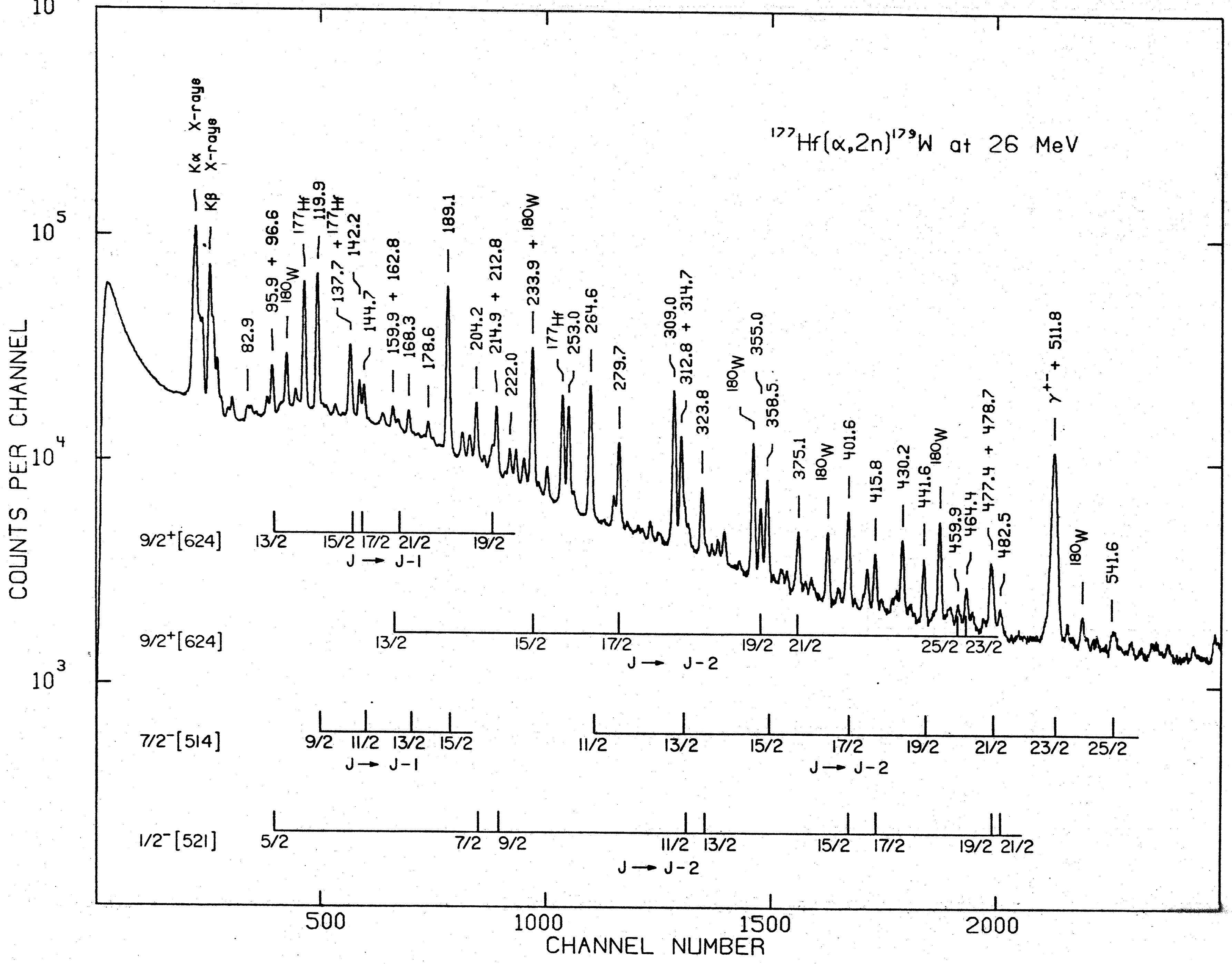

$^{177}Hf(\alpha,2n)^{179}W$ at 26 MeV
COUNTS PER CHANNEL
CHANNEL NUMBER
Kα X-rays
Kβ X-rays
82.9
95.9 + 96.6
180W
177Hf
119.9
137.7 + 177Hf
142.2
144.7
159.9 + 162.8
168.3
178.6
189.1
204.2
214.9 + 212.8
222.0
233.9 + 180W
177Hf
253.0
264.6
279.7
309.0
312.8 + 314.7
323.8
180W
355.0
358.5
375.1
180W
401.6
415.8
430.2
441.6
180W
459.9
464.4
477.4 + 478.7
482.5
γ+- + 511.8
180W
541.6
9/2+[624]
J → J-1
9/2+[624]
J → J-2
7/2-[514]
J → J-1
J → J-2
1/2-[521]
J → J-2

Fig. 2

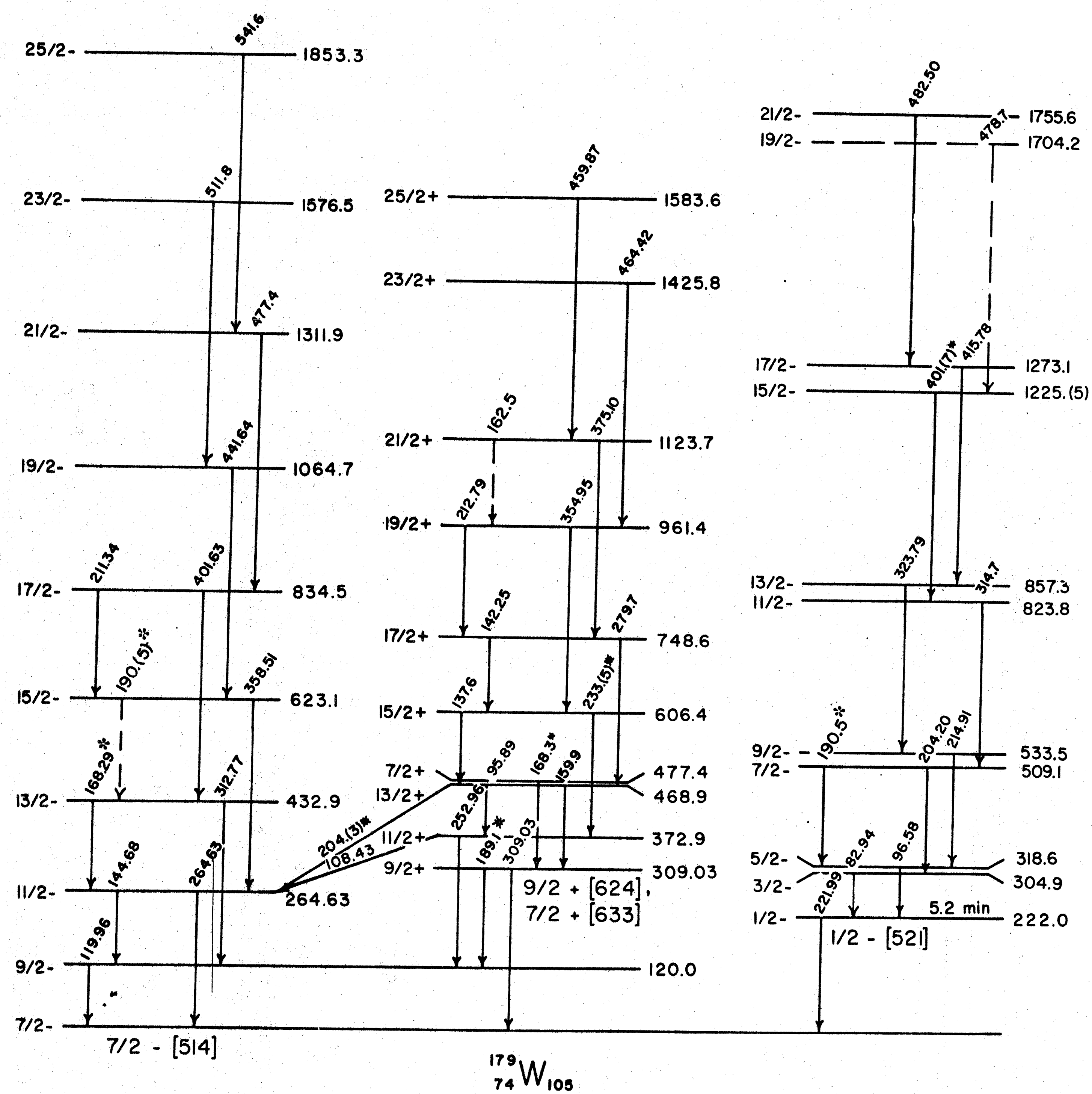
25/2-
1853.3
541.6
23/2-
1576.5
511.8
21/2-
1311.9
477.4
19/2-
1064.7
441.64
17/2-
834.5
211.34
401.63
190.(5)*
15/2-
623.1
358.51
168.29*
13/2-
432.9
312.77
11/2-
144.68
264.63
264.63
119.96
9/2-
7/2-
7/2 - [514]
25/2+
1583.6
459.87
23/2+
1425.8
464.42
21/2+
1123.7
162.5
375.10
19/2+
961.4
212.79
354.95
17/2+
748.6
142.25
279.7
15/2+
606.4
137.6
233.(5)*
7/2+
477.4
13/2+
468.9
95.89
168.3*
159.9
204.(3)*
108.43
11/2+
372.9
252.96
189.1*
309.03
9/2+
309.03
9/2 + [624],
7/2 + [633]
120.0
21/2-
1755.6
482.50
19/2-
1704.2
478.1
17/2-
1273.1
401.(7)*
415.78
15/2-
1225.(5)
13/2-
857.3
11/2-
823.8
323.79
314.7
9/2-
533.5
190.5*
7/2-
509.1
204.20
214.91
5/2-
318.6
3/2-
304.9
82.94
96.58
221.99
1/2-
222.0
5.2 min
1/2 - [521]
$^{179}_{74}W_{105}$

Fig. 3

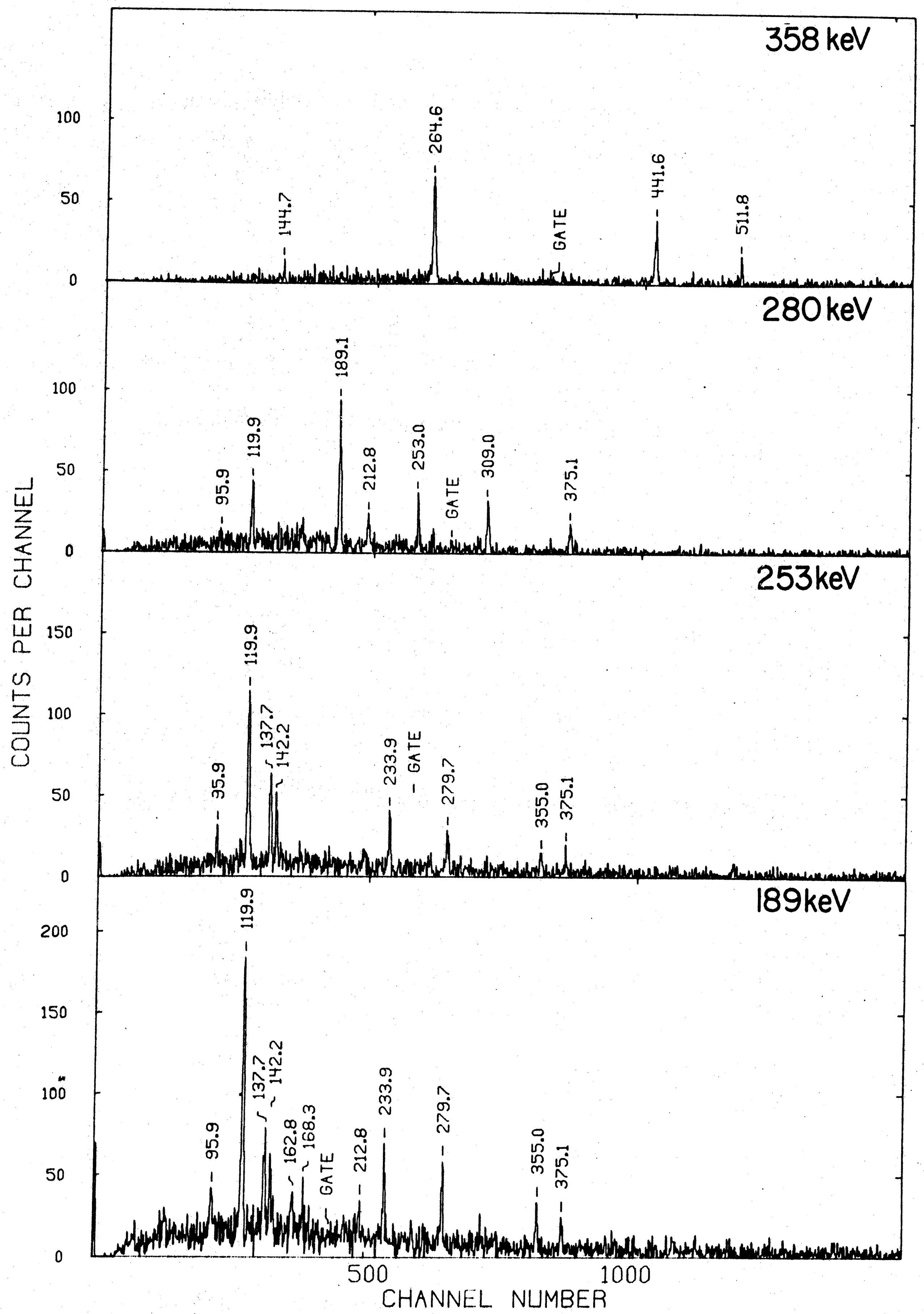
358 keV
144.7
264.6
GATE
441.6
511.8
280 keV
95.9
119.9
189.1
212.8
253.0
GATE
309.0
375.1
253 keV
95.9
119.9
137.7
142.2
233.9
GATE
279.7
355.0
375.1
189 keV
95.9
119.9
137.7
142.2
162.8
168.3
GATE
212.8
233.9
279.7
355.0
375.1
0
50
100
150
200
COUNTS PER CHANNEL
500
1000
CHANNEL NUMBER

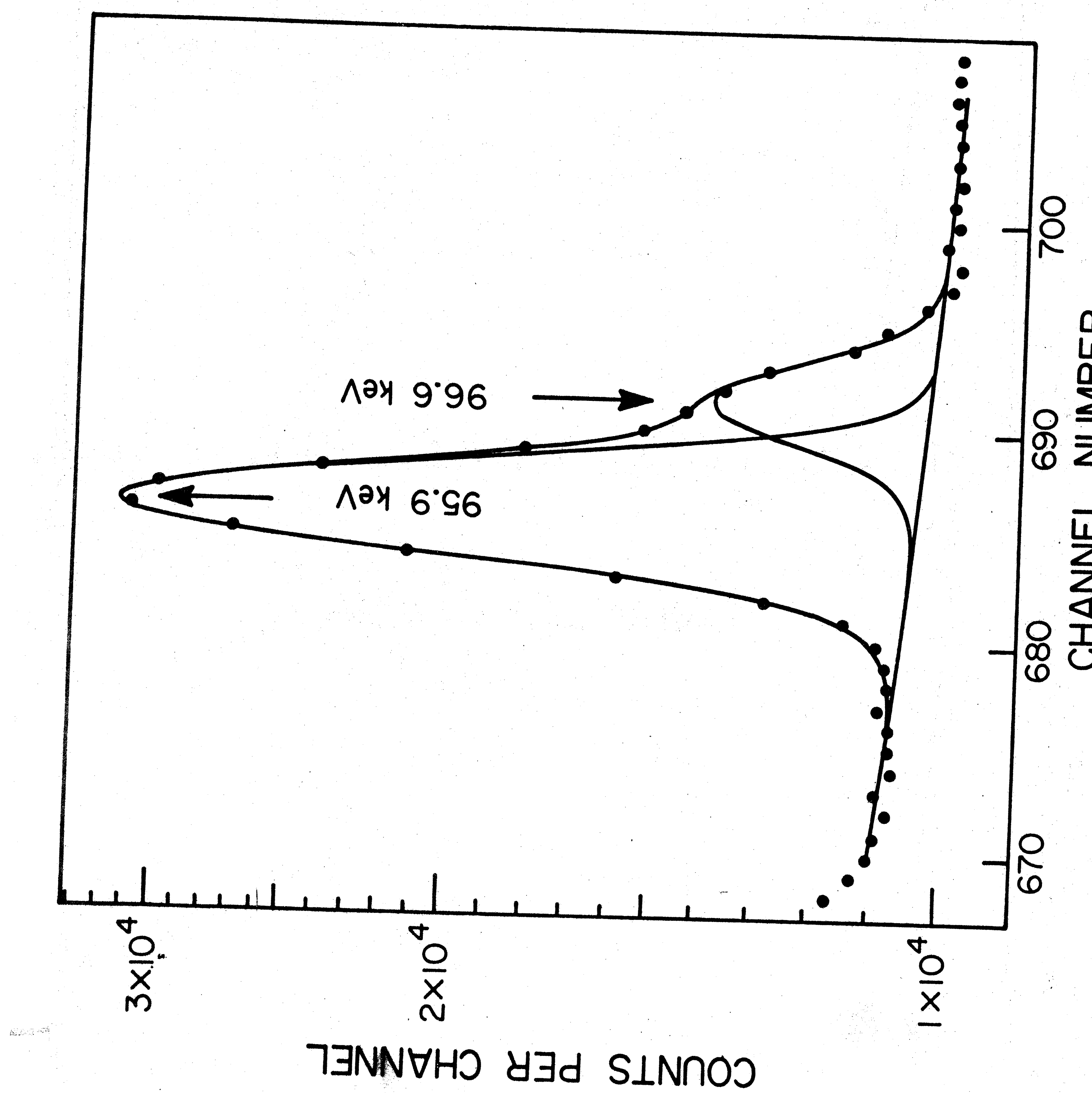
COUNTS PER CHANNEL
3×10⁴
2×10⁴
1×10⁴
CHANNEL NUMBER
670
680
690
700
95.9 keV
96.6 keV

Fig. 5

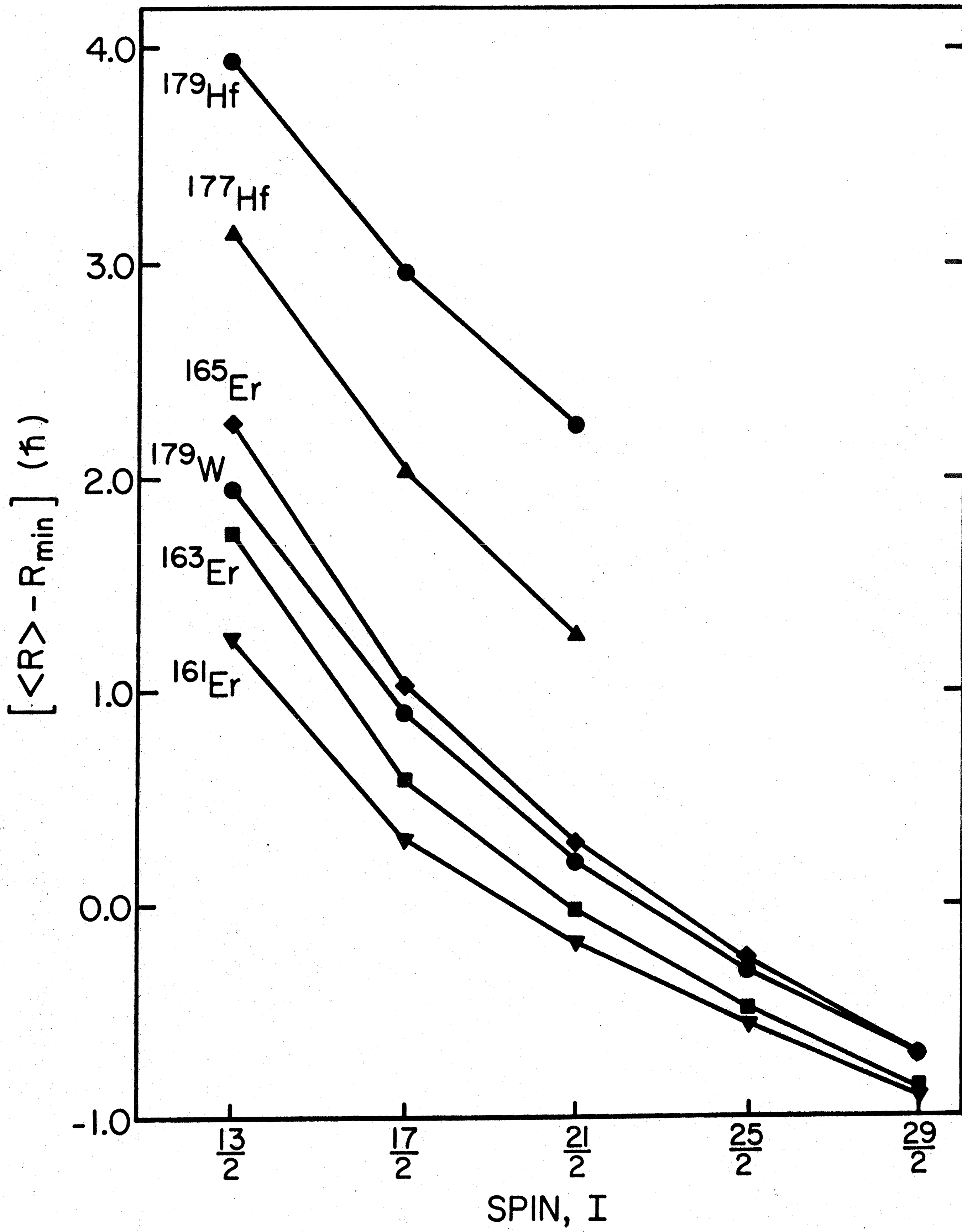
4.0
3.0
2.0
1.0
0.0
-1.0
^{179}Hf
^{177}Hf
^{165}Er
^{179}W
^{163}Er
^{161}Er
$[\langle R\rangle - R_{min}]$ ($\hbar$)
$\frac{13}{2}$
$\frac{17}{2}$
$\frac{21}{2}$
$\frac{25}{2}$
$\frac{29}{2}$
SPIN, I

Fig. 6